Trimerization and orbital ordering in $Ba_{1-x}Sr_xV_{13}O_{18}$

T. Kajita,[1] Y. Obata,[1] Y. Kakesu,[1] Y. Imai,[2] Y. Shmizu,[2] M. Itoh,[2] H. Kuwahara,[3] and T. Katsufuji[1,4]
[1]*Department of Physics, Waseda University, Tokyo 169-8555, Japan*
[2]*Department of Physics, Nagoya University, Chikusa, Nagoya 464-8602, Japan*
[3]*Department of Physics, Sophia University, Tokyo 102-8554, Japan*
[4]*Kagami Memorial Laboratory for Material Science and Technology, Waseda University, Tokyo 169-0051, Japan*
(Received 14 July 2017; revised manuscript received 3 October 2017; published 21 December 2017)

We studied the physical properties of $Ba_{1-x}Sr_xV_{13}O_{18}$ single crystals, which exhibit three different phases caused by the orbital and charge degrees of freedom in V t_{2g} states. We found from the magnetic susceptibility and the NMR measurement that the low-temperature phase of this series of compounds is characterized by the spin-singlet state. We also found from the electrical resistivity and optical conductivity spectra that these compounds become heavily anisotropic in the low-temperature phase with V trimerization, indicating that the orbital ordering of V t_{2g} states causes the anisotropy of the electronic structure of this series of compounds.

DOI: 10.1103/PhysRevB.96.245126

I. INTRODUCTION

Vanadium oxides with one or two d electrons in t_{2g} states exhibit various interesting ordered states arising from the orbital degree of freedom of the d electrons. For example, $LiVO_2$ with V^{3+} ($3d^2$) ions on a triangular lattice exhibits the trimerization of V ions at ∼460 K, causing a sharp decrease in magnetic susceptibility [1–3]. It was proposed by Pen *et al.* that such trimerization is caused by the orbital ordering of t_{2g} states on V ions and the formation of a spin-singlet bond at each edge of the V trimer [4], as shown in Fig. 1(a).

Recently, it has been found that $BaV_{10}O_{15}$ (in which the average valence of V is +2.8) [5–8], $Ba_2V_{13}O_{22}$ (+3.08) [9], and $Ba_{1-x}Sr_xV_{13}O_{18}$ (+2.62) [10–12] with V ions on a quasi-triangular lattice exhibit ordered states similar to that of $LiVO_2$. For example, the trimerization of V ions occurs in $BaV_{10}O_{15}$ at 123 K, causing the opening of a charge gap of ∼0.3 eV and a sharp increase in resistivity by three orders of magnitude [6]. A similar phase transition with V trimerization accompanied by a sharp decrease in magnetic susceptibility is observed in $Ba_2V_{13}O_{22}$ but at a higher temperature of ∼290 K [9].

It should be pointed out that these vanadates with mixed-valent V ions also have the charge degree of freedom of the d electrons, unlike $LiVO_2$ with only V^{3+} ions, and this results in a wider variety of phase transitions. In this respect, $Ba_{1-x}Sr_xV_{13}O_{18}$ with a hexagonal structure, in which V ions form a quasi-fcc lattice, are an intriguing series of compounds since they exhibit three different phases with temperature [10,11], as shown in Fig. 2. For $BaV_{13}O_{18}$, the high-temperature (HT) phase is characterized by magnetic susceptibility χ that decreases with decreasing T and also by a structural distortion, in which six V tetramers in a rhombus shape surround one center V ion, as illustrated in Fig. 1(c). In this V tetramer, there are five V-V bonds, each of which presumably consists of two V t_{2g} states in a spin singlet state [Fig. 1(b)]; namely, the orbital ordering of the V t_{2g} states occurs in this HT phase. With decreasing temperature, the transition from the HT phase to the intermediate-temperature (IT) phase occurs at $T_{co} \sim 200$ K, and the IT phase is characterized by the Curie-Weiss behavior of magnetic susceptibility and the doubling of a unit cell, although the basic structure of the V tetramers is unchanged. These results suggest the charge ordering of the localized d electrons on the center V ion in the IT phase, although there are still itinerant electrons in this phase, as described below. With a further decrease in temperature, another transition from the IT phase to the low-temperature (LT) phase occurs at $T_{tr} \sim 70$ K. In the HT and IT phases, there are three V tetramers and one center V ion in a unit cell (13 V ions), but they change into three V trimers and one V tetramer in the LT phase [Fig. 1(d)]. It is speculated that each bond of a V trimer consists of two V t_{2g} states in a spin-singlet state [Fig. 1(a)] [4]. With increasing Sr concentration x in $Ba_{1-x}Sr_xV_{13}O_{18}$, T_{co} decreases, whereas T_{tr} increases; the IT phase for $T_{tr} < T < T_{co}$ eventually disappears, and the transition from the HT phase to the LT phase occurs in the region of $x > 0.3$. This behavior indicates a competition between the IT and LT phases in this series of compounds.

Previous studies on $Ba_{1-x}Sr_xV_{13}O_{18}$ were performed mainly using polycrystalline samples [10,11], and studies using single crystals were carried out only on $BaV_{13}O_{18}$ [12]. In this study, we investigate the physical properties of $Ba_{1-x}Sr_xV_{13}O_{18}$ single crystals. In particular, we focus on how the anisotropy of the electronic structure changes with different phases and the Sr concentration x.

II. EXPERIMENT

We grew $Ba_{1-x}Sr_xV_{13}O_{18}$ single crystals using the floating-zone technique. Details were described elsewhere [12]. Electrical resistivity was measured using a conventional four-probe method. Magnetic susceptibility was measured using a superconducting quantum interference device magnetometer. The Hall coefficient was measured at applied magnetic fields of up to 7 T by using a superconducting magnet. Optical reflectivity on a cleaved surface along the $(32\bar{2})$ plane was measured using a Fourier transform infrared spectrometer between 0.07 and 0.8 eV and a grating spectrometer between 0.7 and 5 eV for the temperature range between 300 and 30 K with a He-gas-flow cryostat. The optical conductivity spectra $\sigma(\omega)$ were obtained with the Kramers-Kronig transformation of reflectivity spectra with a constant extrapolation of the reflectivity below 0.07 eV and a constant extrapolation between 5 and 20 eV and an ω^{-4} extrapolation above. The way to obtain $\sigma(\omega)$ along the

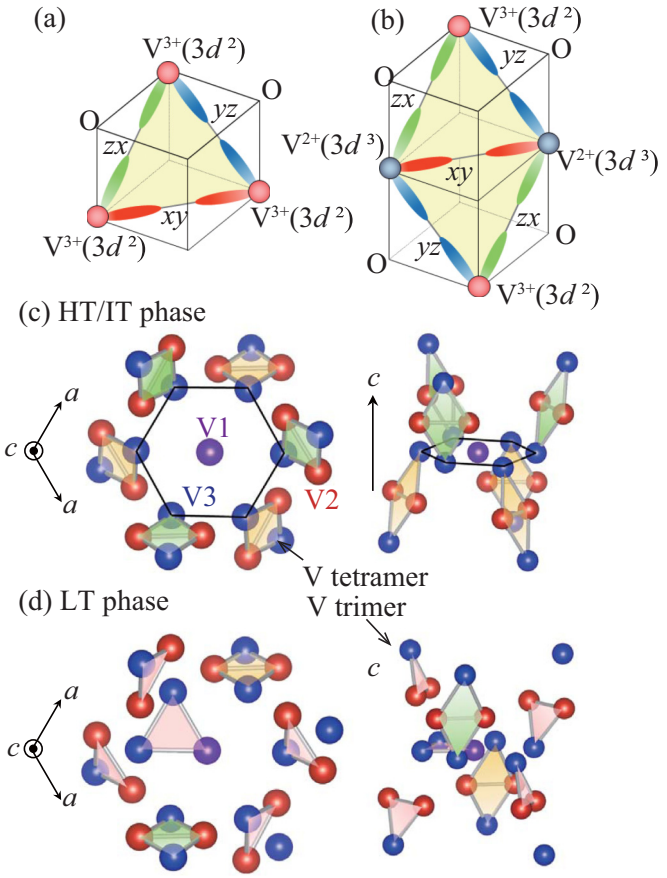

FIG. 1. Schematic illustrations of orbital ordering in (a) the V trimer and (b) V tetramer. (c) Arrangement of V ions in HT and IT phases viewed along the c axis (left) and the ab plane (right). (d) Arrangement of V ions in the LT phase viewed along the c axis (left) and the ab plane (right). (c) and (d) were drawn using VESTA [13].

a and the c axes from the reflectivity spectra on the surface along such an oblique $(32\bar{2})$ plane was described in Ref. [12]. ^{51}V NMR spectra and the nuclear spin-lattice relaxation rate were measured for $x = 0$ and $x = 0.1$ samples at a constant magnetic field of 6.10 T.

III. RESISTIVITY, MAGNETIC SUSCEPTIBILITY, AND HALL MEASUREMENT

Figures 3(a)–3(d) show the resistivity ρ of the $Ba_{1-x}Sr_xV_{13}O_{18}$ single crystals with $x = 0,0.1,0.2$, and 1 along the a axis (ρ_a) and c axis (ρ_c). At 300 K, the magnitudes of ρ_a and ρ_c are comparable, and both increase with decreasing temperature T. When $x \leqslant 0.2$, $\rho_a(T)$ and $\rho_c(T)$ exhibit small anomalies at T_{co} (solid triangles). $\rho_a(T)$ and $\rho_c(T)$ from 300 K to T_{co} can be fitted on the basis of the thermal activation-type T dependence, $\rho = \rho_0 \exp(E_g/k_B T)$, and the activation energy E_g is plotted as a function of x in Fig. 3(f). As can be seen, E_g/k_B is comparable to T_{co}. Below T_{co} in the IT phase, the increases in $\rho_a(T)$ and $\rho_c(T)$ with decreasing T become less significant, and they rather decrease with decreasing T for $x = 0$ and 0.1, typical of a metallic state.

With a further decrease in T when $x \leqslant 0.2$, $\rho_a(T)$ sharply decreases, whereas $\rho_c(T)$ sharply increases with a T hysteresis

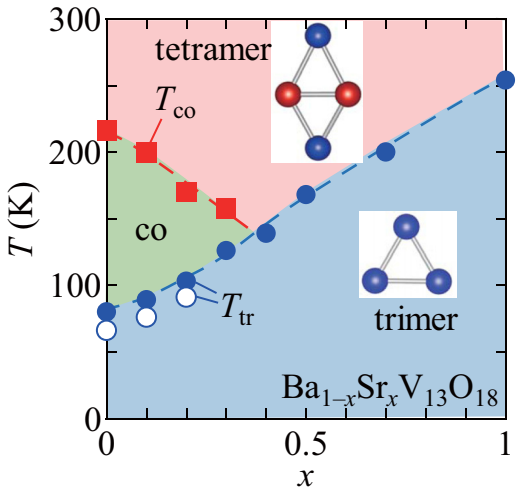

FIG. 2. Phase diagram of the $Ba_{1-x}Sr_xV_{13}O_{18}$ single crystals. The closed squares correspond to the transition temperatures between the HT phase and the IT phase. The circles correspond to the transition temperatures between the IT phase and LT phase ($x \leqslant 0.3$) or between the HT phase and LT phase ($x > 0.3$). The solid and open circles correspond to that in the warming and cooling runs, respectively.

at T_{tr} (open triangles), and below T_{tr} in the LT phase, both $\rho_a(T)$ and $\rho_c(T)$ increase with decreasing T, but the increase is more significant for $\rho_c(T)$. For $SrV_{13}O_{18}$, where T_{co} no longer exists, $\rho_a(T)$ sharply decreases, whereas $\rho_c(T)$ sharply increases at $T_{tr} \sim 250$ K [see the inset of Fig. 3(d)], and ρ_a is almost T independent, whereas ρ_c increases with decreasing T below T_{tr} in the LT phase. Such anisotropic behavior of $\rho(T)$ in the LT phase for $Ba_{1-x}Sr_xV_{13}O_{18}$ will be discussed later together with the anisotropy of optical conductivity. It should be pointed out that the decrease in $\rho(T)$ at T_{tr} with decreasing T for the polycrystalline samples [11] is dominated by the behavior of $\rho_a(T)$ for the single crystals.

Figure 3(e) shows the magnetic susceptibility $\chi(T)$ of the $Ba_{1-x}Sr_xV_{13}O_{18}$ single crystals. As shown for $BaV_{13}O_{18}$, the anisotropy in $\chi(T)$ between $H \parallel a$ (χ_a) and $H \parallel c$ (χ_c) is barely observed in the entire temperature range, unlike that in $\rho(T)$. When $x \leqslant 0.3$, $\chi(T)$ decreases with decreasing T from 300 K to T_{co} in the HT phase. As discussed in the Introduction, this can be attributed to the spin-gap behavior dominated by the thermal excitation from the spin-singlet state to the spin-triplet state in the V-V bonds of the V tetramers [Fig. 1(c)].

At T_{co} (solid triangles), $\chi(T)$ exhibits a small drop, and below T_{co} in the IT phase, it obeys the Curie-Weiss behavior, which can be attributed to the local magnetic moment at the center V ion. To estimate the local magnetic moment in the IT phase of $Ba_{1-x}Sr_xV_{13}O_{18}$ ($x = 0$, 0.1, and 0.2), $\chi(T)$ was fitted using $\chi(T) = \chi_v + C/(T + \theta)$, where χ_v is a T-independent paramagnetic term (Van Vleck term) and the second term is a Curie-Weiss term with the Curie constant C and the Weiss temperature θ. The χ_v value of $\sim 1 \times 10^{-4}$ cm^3/V mol is comparable to those of $LiVO_2$ [14] and V_2O_3 [15]. The Curie constant C obtained by fitting is in the range of 1.1–1.5 $\times 10^{-2}$ cm^3 K/V mol for $x = 0$–0.2.

At T_{tr} (open triangle), $\chi(T)$ sharply decreases and shows an almost T-independent behavior below T_{tr}, although a small Curie term appears below 30 K. This sharp decrease in

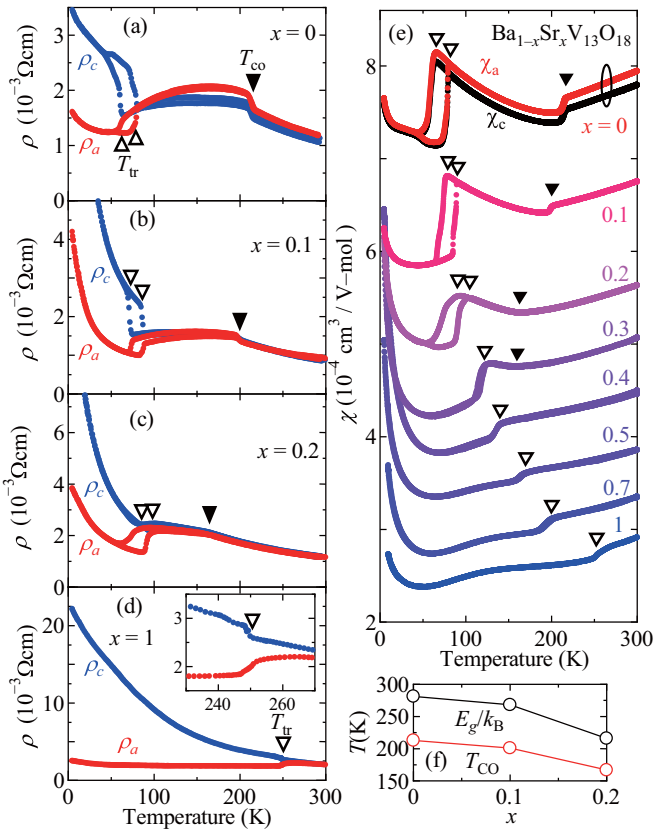

FIG. 3. Temperature dependence of the resistivity for $Ba_{1-x}Sr_xV_{13}O_{18}$ with (a) $x = 0$, (b) $x = 0.1$, (c) $x = 0.2$, and (d) $x = 1$. (e) Temperature dependence of the magnetic susceptibility for $Ba_{1-x}Sr_xV_{13}O_{18}$. The data are offset for clarity. (f) Sr concentration dependences of E_g/k_B and T_{co}.

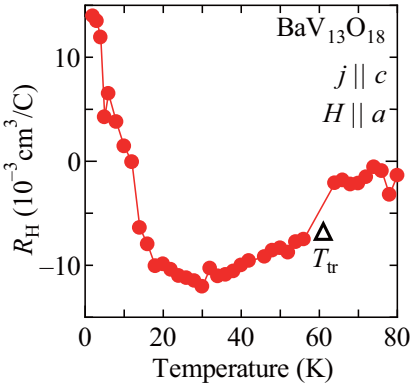

FIG. 4. Temperature dependence of the Hall coefficient for $BaV_{13}O_{18}$.

$\chi(T)$ at T_{tr}, which is much more prominent than that for the polycrystalline samples [11] and is accompanied by a T hysteresis, is caused by V trimerization and the suppression of the magnetic moment on the center V ion.

With increasing x for $Ba_{1-x}Sr_xV_{13}O_{18}$, T_{co} decreases, whereas T_{tr} increases, and when $x \geqslant 0.4$, T_{co} and T_{tr} merge, and the Curie-Weiss behavior disappears. We draw the phase diagram of the $Ba_{1-x}Sr_xV_{13}O_{18}$ single crystals in Fig. 2, where T_{co} and T_{tr} are obtained from the magnetic susceptibility data. The result is similar to that of the polycrystalline samples previously reported [11], except for the behavior at $x = 0$. In the case of the polycrystalline samples, although T_{tr} exists in $Ba_{1-x}Sr_xV_{13}O_{18}$ with finite values of x, no anomaly corresponding to T_{tr} was observed for $BaV_{13}O_{18}$ [11]. According to the studies on the single crystals, the stoichiometric $BaV_{13}O_{18}$ crystal exhibits T_{tr}, whereas the off-stoichiometric one does not [12]. It is likely that this results in the different behaviors at $x = 0$ between the polycrystalline samples and the single crystals.

The Hall coefficient R_H with $j \parallel c$ and $H \parallel a$ for $BaV_{13}O_{18}$ as a function of T is shown in Fig. 4. R_H above T_{tr} (in the IT phase) is negative, and the absolute value immediately above $T_{tr} = 60$ K is $\sim 2 \times 10^{-3}$ cm^3/C, which corresponds to 0.07 electron per V ion. In $Ba_{1-x}Sr_xV_{13}O_{18}$, there are 31 d electrons per 13 V ions, and in the IT phase, 30 electrons can be accommodated in the three V tetramers (each of which has five bonds and can accommodate ten electrons); thus, one d electron should exist on the center V ion. However, part of this electron should be localized and contributes to the Curie-Weiss behavior of magnetic susceptibility. Thus, one possible scenario for the IT phase is that some d electrons on the center V ion are localized and contribute to the Curie-Weiss behavior, whereas the others are itinerant and contribute to the Hall coefficient. The doubling of the unit cell observed in the electron diffraction [10] seems to support this idea. Furthermore, the Curie constant experimentally obtained (1.1–1.5 $\times 10^{-2}$ cm^3 K/V mol) is comparable to that obtained when a $S = 1/2$ spin exists per doubled unit cell (26 V), $C = 1.4 \times 10^{-2}$ cm^3 K/V mol. The number of itinerant electrons in the IT phase estimated from the Hall coefficient above T_{tr} ($\sim$0.07) seems compatible with the number of carriers in this model, $1/26 \sim 0.038$.

With decreasing T, R_H sharply drops to -8×10^{-3} cm^3/C at 56 K (immediately below $T_{tr} = 60$ K), and with a further decrease in T, R_H starts to increase below 20 K, and the sign of R_H changes from negative to positive at 12 K and reaches 1.4×10^{-2} cm^3/C at the lowest temperature of 2 K. The change in sign indicates that, in the LT phase, two kinds of carriers, namely, holes and electrons, exist. In the case of charge-density-wave (CDW) compounds [16,17], the sign of the Hall coefficient changes from positive to negative at the CDW phase transition accompanied by nesting of the Fermi surface. In Ru oxides, such as Sr_2RuO_4 [18–20], $SrRuO_3$ [21], and $Ba_4Ru_3O_{10}$ [22], the complicated band structures cause the sign inversion of the Hall coefficient with temperature.

The number of carriers estimated from R_H at 56 K is $\sim$0.02 electron per V ion. In the LT phase, there are 31 d electrons per 13 V ions, and 28 electrons can be accommodated in one V tetramer (which can accommodate ten electrons) and three V trimers (each of which can accommodate six electrons). Thus, three electrons do not form a bonding state and should be itinerant. However, the number of electrons per V ion experimentally estimated ($\sim$0.02) is much smaller than that expected from such a simple model discussed above, $3/13 \sim 0.23$. Furthermore, this model cannot explain the existence of both holes and electrons. These two results suggest that complex Fermi surfaces exist in the LT phase of this series of compounds.

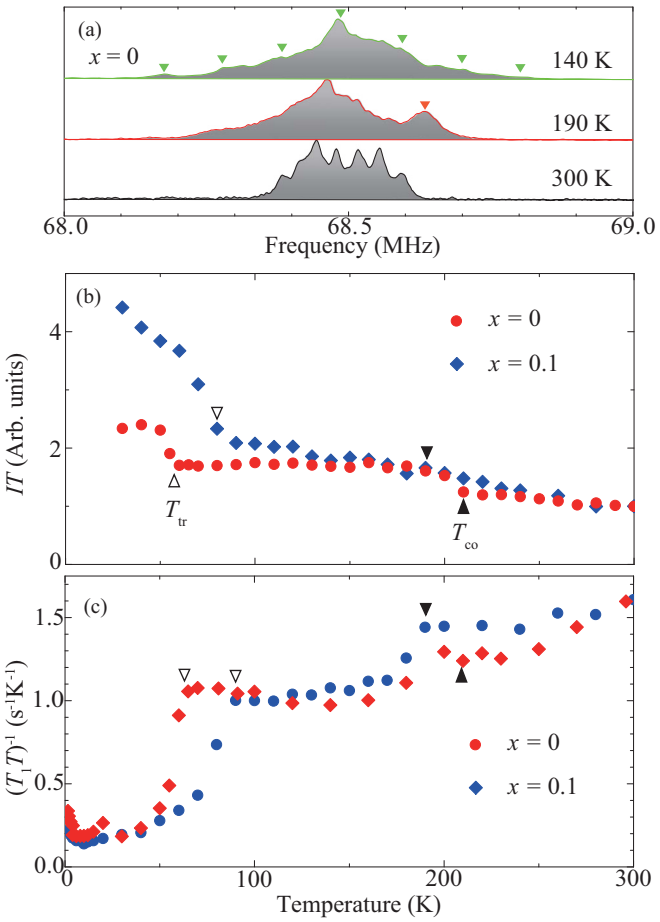

FIG. 5. (a) ^{51}V NMR spectra of $BaV_{13}O_{18}$ for $H \parallel c$. The intensity of the spectra is normalized using the peak value. The Knight shift origin ($K = 0$) is located at 68.264 MHz for $H = 6.10$ T. The green inverse triangles represent the electric quadrupole splitting. (b) Temperature T dependence of integrated spin-echo intensity I multiplied by T, where I is extrapolated to $\tau = 0$ by measuring the spin-echo decay rate T_2^{-1} using the pulse sequence of $(\pi/2)$-τ-$(\pi/2)$-τ, and (c) nuclear spin-lattice relaxation rate T_1^{-1} divided by T for $x = 0$ and $x = 0.1$.

IV. NMR MEASUREMENT

To obtain microscopic insights into the ground state, the ^{51}V NMR spectrum was measured on the single crystal of the $x = 0$ sample for a magnetic field of 6.10 T along the c axis,

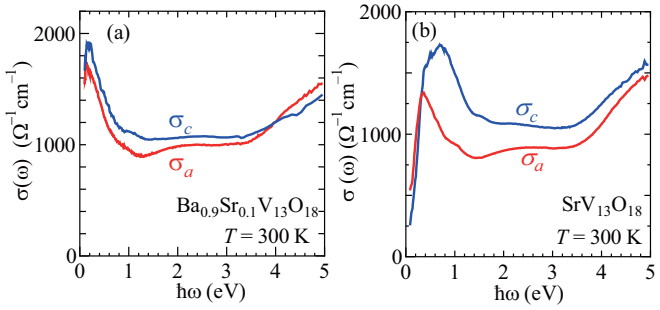

FIG. 6. Optical conductivity spectra along the ab plane [$\sigma_a(\omega)$] and c axis [$\sigma_c(\omega)$] at 300 K for (a) $Ba_{0.9}Sr_{0.1}V_{13}O_{18}$ and (b) $SrV_{13}O_{18}$.

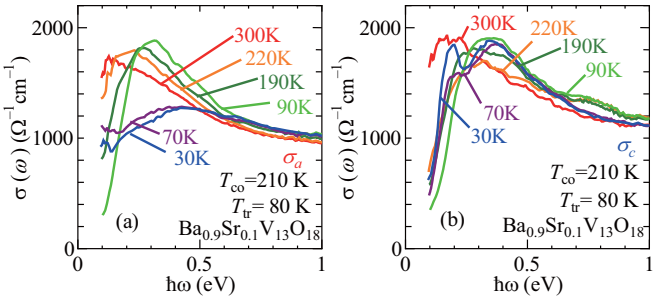

FIG. 7. Optical conductivity spectra along (a) the ab plane [$\sigma_a(\omega)$] and (b) the c axis [$\sigma_c(\omega)$] for $Ba_{0.9}Sr_{0.1}V_{13}O_{18}$ at various temperatures.

as shown in Fig. 5(a). We observed one set of nonmagnetic NMR spectra with small quadrupole splitting for the nuclear spin $I = 7/2$ at 300 K. The observed nonmagnetic V site can be V2 among the tetramers in the HT phase since the V2-V2 bond is much shorter than the V2-V3 bond. The spectra from V1 and V3 are wiped out due to the fast nuclear spin relaxation rates in the HT phase. The shape of the spectrum clearly changes across T_{co} and T_{tr}. At 190 K below T_{co}, the spectrum becomes complex with the decrease in symmetry. An additional line at the higher-frequency side [the red inverse triangle in Fig. 5(a)] possibly originates from some of the V3 sites, which become nonmagnetic through the formation of a strong trimer or tetramer. Below T_{tr}, the quadrupole splitting is enhanced and partly resolved with a splitting frequency of 0.1 MHz, which suggests d orbital ordering.

Unlike in the case of bulk susceptibility, a weak temperature variation is observed in the Knight shift for the main peak. Therefore, the observed V sites (V2) have vanishing spin susceptibility, and the other V sites (V1 and V3) dominate the bulk susceptibility. The integrated spectral intensity I multiplied by temperature T abruptly increases below T_{tr} [Fig. 5(b)]. This means that the number of nonmagnetic V sites increases below T_{tr}, consistent with the suppression of bulk susceptibility. We observed a similar behavior for $x = 0.1$.

The nuclear spin-lattice relaxation rate divided by temperature $(T_1T)^{-1}$ is a measure of the density of states N in Korringa's law for itinerant systems, $(T_1T)^{-1} \propto N^2$. As shown in Fig. 5(c), we observed a constant behavior of $(T_1T)^{-1}$ for each phase and a stepwise decrease in $(T_1T)^{-1}$ across the phase transitions. In the LT phase, $(T_1T)^{-1}$ is suppressed to

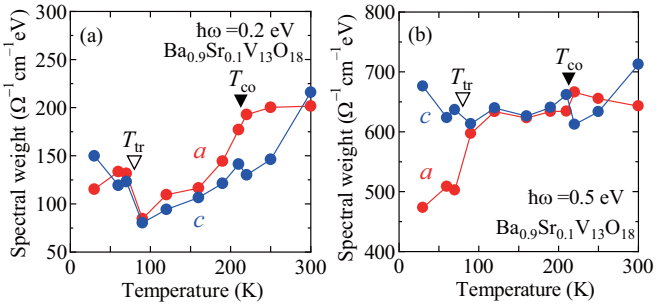

FIG. 8. Temperature dependence of the spectral weight (a) between 0.1 and 0.2 eV and (b) between 0.1 and 0.5 eV.

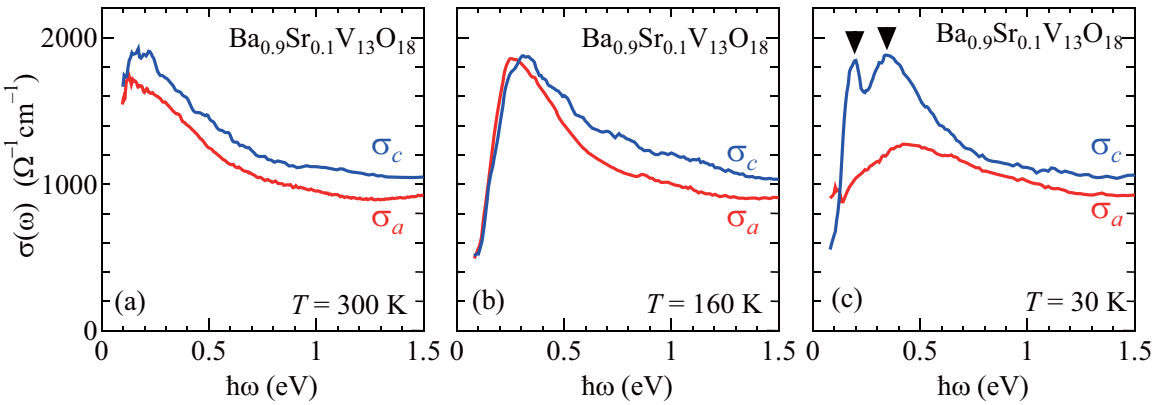

FIG. 9. The $\sigma_a(\omega)$ and $\sigma_c(\omega)$ spectra at (a) 300 K (HT phase), (b) 160 K (IT phase), and (c) 30 K (LT phase).

~10% of the HT phase value, corresponding to the residual density of states of ~30%. This result supports the reduction in carrier (electron) density through valence-bond formations of all V sites and orbital ordering at T_{tr}, as exemplified in the T dependence of the Hall coefficient (Fig. 4).

V. OPTICAL MEASUREMENT

Figures 6(a) and 6(b) show the optical conductivity spectra along the ab plane [$\sigma_a(\omega)$] and the c axis [$\sigma_c(\omega)$] for $Ba_{0.9}Sr_{0.1}V_{13}O_{18}$ (exhibiting the HT, IT, and LT phases) and $SrV_{13}O_{18}$ (exhibiting the HT and LT phases) at 300 K up to 5 eV, respectively. There are three structures in all the spectra. The peak below 1 eV can be assigned to the excitation of the d electrons between V ions with different valences [mainly from V^{2+} ($3d^3$) to V^{3+} ($3d^2$)], which is called in-gap excitation. The broad peak centered at 2 eV can be assigned to the Mott-gap excitation, which is the excitation of the d electrons between V ions with the same valence [mainly from V^{3+} ($3d^2$) to V^{3+} ($3d^2$)]. The structures above 3.5 eV can be attributed to the charge-transfer excitation, which is the excitation from the oxygen $2p$ state to the V d state. This is similar to the spectrum for $BaV_{13}O_{18}$ (exhibiting only the HT and IT phases) previously reported [12].

Figures 7(a) and 7(b) show the $\sigma_a(\omega)$ and $\sigma_c(\omega)$ spectra of $Ba_{0.9}Sr_{0.1}V_{13}O_{18}$ below 1 eV at various temperatures. With decreasing T, the peak at ~0.1 eV in both $\sigma_a(\omega)$ and $\sigma_c(\omega)$ shifts to a higher frequency across T_{co} (from the HT phase to the IT phase). This spectral change is similar to that of $BaV_{13}O_{18}$, exhibiting only the HT and IT phases previously reported [12]. With a further decrease in T, the peak in $\sigma_a(\omega)$ (0.3 eV at 90 K) decreases and broadens below $T_{tr} = 80$ K (from the IT phase to the LT phase). With this peak broadening, $\sigma_a(\omega)$ below 0.1 eV increases below T_{tr}. This is consistent with the decrease in $\rho_a(T)$ (increase in dc conductivity) below T_{tr} [Fig. 3(b)]. On the other hand, the peak in $\sigma_c(\omega)$ (~0.4 eV at 90 K) splits into two peaks at 0.2 and 0.4 eV, but the suppression of the spectral weight at low frequencies survives even below T_{tr}, consistent with the increase in $\rho_c(T)$ below T_{tr} [Fig. 3(b)].

To see the change in electronic structure more clearly, the spectral weights for $Ba_{0.9}Sr_{0.1}V_{13}O_{18}$ were obtained by integrating $\sigma_a(\omega)$ and $\sigma_c(\omega)$ between 0.1 and 0.2 eV and between 0.1 and 0.5 eV and are plotted as a function of T in Figs. 8(a) and 8(b). The spectral weight for $\sigma_a(\omega)$ up to 0.2 eV begins to decrease below T_{co} [Fig. 8(a)], whereas that for both $\sigma_a(\omega)$ and $\sigma_c(\omega)$ up to 0.5 eV barely changes at T_{co} [Fig. 8(b)]. With a further decrease in T, the spectral weight for $\sigma_a(\omega)$ up to 0.5 eV decreases at T_{tr} [Fig. 8(b)]. These results indicate that the spectral weight transfer associated with the transition from the HT phase to the IT phase occurs only below 0.5 eV, whereas that with the transition from the IT phase to the LT phase extends over the energy scale higher than 0.5 eV. Note that a similar change in the optical conductivity spectrum

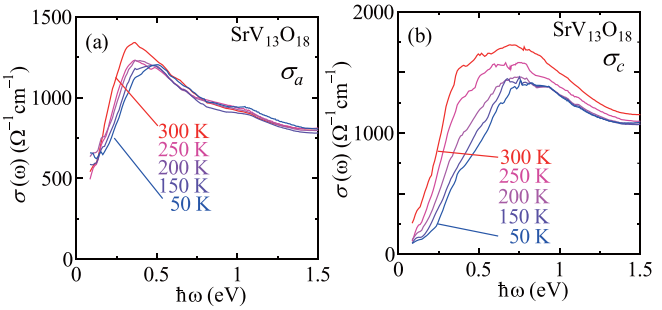

FIG. 10. (a) The $\sigma_a(\omega)$ and (b) $\sigma_c(\omega)$ spectra for $SrV_{13}O_{18}$ at various temperatures.

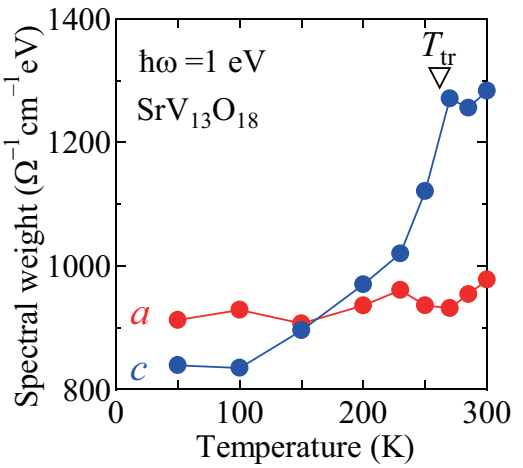

FIG. 11. Temperature dependence of spectral weight for $\sigma_a(\omega)$ (red circles) and $\sigma_c(\omega)$ (blue circles) between 0.1 and 1 eV.

over an energy scale much higher than 0.5 eV is observed in $BaV_{10}O_{15}$ [6], which exhibits a phase transition with the V trimerization caused by the orbital ordering of V t_{2g} states, similar to the LT phase in the present compound.

To see the anisotropy of optical conductivity, the $\sigma_a(\omega)$ and $\sigma_c(\omega)$ spectra at the same temperature (300, 160, or 30 K) for $Ba_{0.9}Sr_{0.1}V_{13}O_{18}$ are compared in the same panel in Fig. 9. As can be seen, $\sigma_a(\omega)$ and $\sigma_c(\omega)$ are similar at 300 K (in the HT phase) and 160 K (in the IT phase), but the peak in $\sigma_c(\omega)$ below 1 eV is discernibly higher than that in $\sigma_a(\omega)$ at 30 K (in the LT phase). As discussed above, the optical conductivity spectra below 1 eV should be attributed to the in-gap excitation between V ions with different valences. Such an excitation is possible within the V tetramer consisting of V^{2+} and V^{3+} [Fig. 1(b)] but not within the V trimer consisting of only V^{3+} ions [Fig. 1(a)]. In the LT phase, the three V trimers do not contribute to the in-gap excitation, and only the V tetramer does. Since the normal axis of the tetramer is away from the c axis by $\sim 70^\circ$ [Fig. 1(d)], the spectral weight for the in-gap excitation is expected to be larger for $\sigma_c(\omega)$. This can explain the peak in $\sigma_c(\omega)$ being larger than that in $\sigma_a(\omega)$ below 1 eV. On the other hand, the nearly isotropic spectra in the IT and HT phases indicate that, although the charge and orbital ordering occurs also in the V tetramer in the IT and HT phases, the charge and orbital modulations are not as large as those in the LT phase for $Ba_{0.9}Sr_{0.1}V_{13}O_{18}$. The appearance of anisotropy in the optical spectra associated with charge/orbital ordering has been observed in various compounds, for example, Ru oxides [23,24], V oxides [25–27], and Mn oxides [28–31].

Note that the anisotropy of the peak in the conductivity spectrum below 1 eV in the LT phase shown in Fig. 9(c) ($\sigma_c > \sigma_a$) is opposite that in the dc resistivity ($\rho_c > \rho_a$) shown in Fig. 3(b). The latter is consistent with the $\sigma_c(\omega)$ and $\sigma_a(\omega)$ spectra that cross at $\sim$0.1 eV and the relation $\sigma_a(\omega) > \sigma_c(\omega)$ below 0.1 eV. This indicates that the itinerant carriers that contribute to the dc conduction and the in-gap excitation between V^{2+} and V^{3+} in the V tetramer have different origins. It was proposed in Ref. [10] that the V-V bonds in the V trimer and V tetramer and the one-dimensional band along the ab plane composed of the d states in the V ions that do not contribute to the bond formation can coexist in the LT phase of this series of compounds. Such a one-dimensional band could explain the lower dc resistivity along the ab plane experimentally observed.

Figures 10(a) and 10(b) show the optical conductivity spectra of $SrV_{13}O_{18}$, which exhibit the transition from the HT phase to the LT phase at $T_{tr} = 270$ K (without the IT phase), at various temperatures. With decreasing T, the peak at $\sim$0.3 eV in $\sigma_a(\omega)$ gradually decreases, but $\sigma_a(\omega)$ below 0.15 eV remains as it is or, rather, increases. On the other hand, in $\sigma_c(\omega)$, the peaks at $\sim$0.3 and $\sim$0.7 eV gradually decrease with decreasing T, and the spectral weight below $\sim$0.2 eV is suppressed at 50 K. This result is consistent with the resistivity behavior; ρ_c continuously increases below T_{tr}, whereas ρ_a is almost T independent.

The spectral weight for $SrV_{13}O_{18}$ between 0.1 and 1 eV is plotted as a function of T in Fig. 11. At T_{tr}, the spectral weight for $\sigma_c(\omega)$ starts to decrease, whereas that for $\sigma_a(\omega)$ is almost T independent. This result indicates that the reconstruction of the electronic structure with the V trimerization occurs over

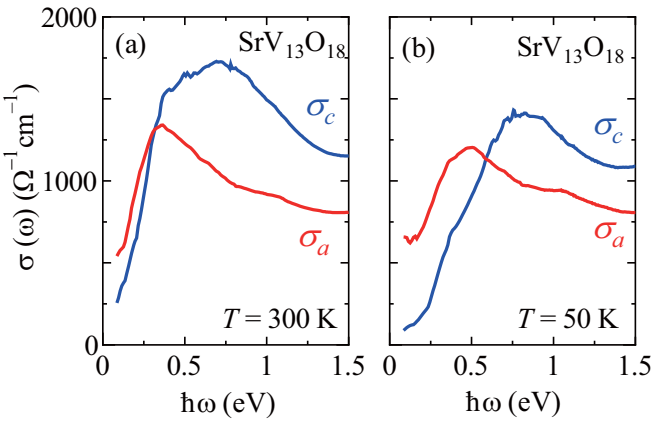

FIG. 12. The $\sigma_a(\omega)$ and $\sigma_c(\omega)$ spectra at (a) 300 K (HT phase) and (b) 50 K (LT phase) for $SrV_{13}O_{18}$.

1 eV in $SrV_{13}O_{18}$, whose energy scale is higher than that in $Ba_{0.9}Sr_{0.1}V_{13}O_{18}$.

The $\sigma_a(\omega)$ and $\sigma_c(\omega)$ spectra at the same T [300 K (HT phase) and 50 K (LT phase)] for $SrV_{13}O_{18}$ are compared in Fig. 12. At 50 K (in the LT phase), the peak in σ_c is larger than that in σ_a, similar to that observed in $Ba_{0.9}Sr_{0.1}V_{13}O_{18}$. However, $\sigma_c(\omega)$ is larger than $\sigma_a(\omega)$ above 0.2 eV even in the HT phase for $SrV_{13}O_{18}$, and this is in contrast to the nearly isotropic spectra in the HT and IT phases for $Ba_{0.9}Sr_{0.1}V_{13}O_{18}$. This is possibly explained by the fact that the V-V bonds in the V tetramer of $SrV_{13}O_{18}$ are shorter than those of $Ba_{0.9}Sr_{0.1}V_{13}O_{18}$ because of the smaller lattice constants (caused by the smaller ionic radius of Sr), giving rise to the larger charge and orbital modulations in the V tetramer and the anisotropy of the electronic structure of $SrV_{13}O_{18}$.

Finally, let us compare the optical conductivity spectra of $Ba_{0.9}Sr_{0.1}V_{13}O_{18}$ and $SrV_{13}O_{18}$ at the lowest T (Fig. 13). The $\sigma_c(\omega)$ spectra of both $Ba_{0.9}Sr_{0.1}V_{13}O_{18}$ and $SrV_{13}O_{18}$ exhibit similar suppression of the spectral weight at low frequencies, but the energy scale in the suppression of $\sigma_c(\omega)$ is discernibly larger for $SrV_{13}O_{18}$. Furthermore, the two peaks at 0.2 and 0.4 eV in the $\sigma_c(\omega)$ spectrum for $Ba_{0.9}Sr_{0.1}V_{13}O_{18}$ shift to higher frequencies at 0.4 and 0.8 eV for $SrV_{13}O_{18}$. As discussed above, the conductivity spectrum in this frequency range is dominated by the in-gap excitation between V^{2+} and V^{3+} existing in the V tetramer. We speculate that the shorter V-V bonds in the V tetramer in $SrV_{13}O_{18}$

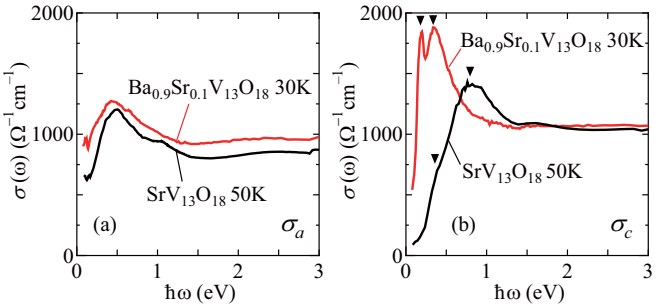

FIG. 13. Comparison of (a) $\sigma_a(\omega)$ and (b) $\sigma_c(\omega)$ at the lowest temperature between $Ba_{0.9}Sr_{0.1}V_{13}O_{18}$ and $SrV_{13}O_{18}$.

than in $Ba_{0.9}Sr_{0.1}V_{13}O_{18}$ cause the larger charge and orbital modulations, resulting in a larger charge gap. On the other hand, the $\sigma_a(\omega)$ spectra of $Ba_{0.9}Sr_{0.1}V_{13}O_{18}$ and $SrV_{13}O_{18}$ are similar up to 3 eV. These behaviors are consistent with those of $\rho_a(T)$ and $\rho_c(T)$ shown in Fig. 3; ρ_c at the lowest T varies from 3×10^{-3} Ω cm to 20×10^{-3} Ω cm with x, whereas ρ_a is within 2–4 $\times 10^{-3}$ Ω cm irrespective of x.

VI. SUMMARY

We measured the electrical resistivity, Hall coefficient, magnetic susceptibility, NMR, and optical reflectivity of $Ba_{1-x}Sr_xV_{13}O_{18}$ single crystals, which have orbital and charge degrees of freedom and exhibit three phases (HT, IT, and LT phases) for $x \leqslant 0.3$ and two phases (HT and LT phases) for $x > 0.3$. We found large changes in various quantities with a phase transition into the LT phase. We also found that anisotropy in the electronic structure is enhanced in the LT phase. These results can be attributed to the orbital ordering of the V t_{2g} states associated with the formation of the V tetramers and trimers in the LT phase of this series of compounds.

ACKNOWLEDGMENTS

This work was supported by JSPS KAKENHI Grant No. JP16H04020, and JP16H04012, and by JST CREST Grant No. JPMJCR15Q2.

[1] P. F. Bonger, Ph.D. Thesis, University of Leiden, 1957.
[2] K. Kobayashi, K. Kosuge, and S. Kachi, Mater. Res. Bull. **4**, 95 (1969).
[3] W. Tian, M. Chisholm, P. Khalifah, R. Jin, B. Sales, S. Nagler, and D. Mandrus, Mater. Res. Bull. **39**, 1319 (2004).
[4] H. F. Pen, J. van den Brink, D. I. Khomskii, and G. A. Sawatzky, Phys. Rev. Lett. **78**, 1323 (1997).
[5] C. Bridges and J. Greedan, J. Solid State Chem. **177**, 1098 (2004).
[6] T. Kajita, T. Kanzaki, T. Suzuki, J. E. Kim, K. Kato, M. Takata, and T. Katsufuji, Phys. Rev. B **81**, 060405(R) (2010).
[7] Y. Shimizu, K. Matsudaira, M. Itoh, T. Kajita, and T. Katsufuji, Phys. Rev. B **84**, 064421 (2011).
[8] K. Takubo, T. Kanzaki, Y. Yamasaki, H. Nakao, Y. Murakami, T. Oguchi, and T. Katsufuji, Phys. Rev. B **86**, 085141 (2012).
[9] J. Miyazaki, K. Matsudaira, Y. Shimizu, M. Itoh, Y. Nagamine, S. Mori, J. E. Kim, K. Kato, M. Takata, and T. Katsufuji, Phys. Rev. Lett. **104**, 207201 (2010).
[10] M. Ikeda, Y. Nagamine, S. Mori, J. E. Kim, K. Kato, M. Takata, and T. Katsufuji, Phys. Rev. B **82**, 104415 (2010).
[11] M. Ikeda, T. Okuda, K. Kato, M. Takata, and T. Katsufuji, Phys. Rev. B **83**, 134417 (2011).
[12] T. Kanzaki, J. Fujioka, Y. Tokura, H. Kuwahara, and T. Katsufuji, Phys. Rev. B **89**, 140401 (2014).
[13] K. Momma and F. Izumi, J. Appl. Crystallogr. **44**, 1272 (2011).
[14] T. Jin-no, Y. Shimizu, M. Itoh, S. Niitaka, and H. Takagi, Phys. Rev. B **87**, 075135 (2013).
[15] E. D. Jones, Phys. Rev. **137**, A978 (1965).
[16] H. N. S. Lee, H. McKinzie, D. S. Tannhauser, and A. Wold, J. Appl. Phys. **40**, 602 (1969).
[17] M. Naito and S. Tanaka, J. Phys. Soc. Jpn. **51**, 219 (1982).
[18] N. Shirakawa, K. Murata, Y. Nishihara, S. Nishizaki, Y. Maeno, T. Fujita, J. G. Bednorz, F. Lichtenberg, and N. Hamada, J. Phys. Soc. Jpn. **64**, 1072 (1995).
[19] A. P. Mackenzie, N. E. Hussey, A. J. Diver, S. R. Julian, Y. Maeno, S. Nishizaki, and T. Fujita, Phys. Rev. B **54**, 7425 (1996).
[20] L. M. Galvin, R. S. Perry, A. W. Tyler, A. P. Mackenzie, S. Nakatsuji, and Y. Maeno, Phys. Rev. B **63**, 161102 (2001).
[21] G. Cao, S. McCall, M. Shepard, J. E. Crow, and R. P. Guertin, Phys. Rev. B **56**, 321 (1997).
[22] Y. Klein, G. Rousse, F. Damay, F. Porcher, G. André, and I. Terasaki, Phys. Rev. B **84**, 054439 (2011).
[23] S. J. Moon, W. S. Choi, S. J. Kim, Y. S. Lee, P. G. Khalifah, D. Mandrus, and T. W. Noh, Phys. Rev. Lett. **100**, 116404 (2008).
[24] C. Mirri, L. Baldassarre, S. Lupi, M. Ortolani, R. Fittipaldi, A. Vecchione, and P. Calvani, Phys. Rev. B **78**, 155132 (2008).
[25] S. Miyasaka, Y. Okimoto, and Y. Tokura, J. Phys. Soc. Jpn. **71**, 2086 (2002).
[26] J. Fujioka, S. Miyasaka, and Y. Tokura, Phys. Rev. Lett. **97**, 196401 (2006).
[27] J. Fujioka, S. Miyasaka, and Y. Tokura, Phys. Rev. B **77**, 144402 (2008).
[28] T. Ishikawa, T. Kimura, T. Katsufuji, and Y. Tokura, Phys. Rev. B **57**, R8079(R) (1998).
[29] T. Ishikawa, K. Tobe, T. Kimura, T. Katsufuji, and Y. Tokura, Phys. Rev. B **62**, 12354 (2000).
[30] J. H. Jung, D.-W. Kim, T. W. Noh, H. C. Kim, H.-C. Ri, S. J. Levett, M. R. Lees, D. M. Paul, and G. Balakrishnan, Phys. Rev. B **64**, 165106 (2001).
[31] K. Tobe, T. Kimura, and Y. Tokura, Phys. Rev. B **69**, 014407 (2004).